3-12-2015

Collectivization of Vascular Smooth Muscle Cells via TGF-β-Cadherin-11-Dependent Adhesive Switching.

Brittany Balint

Hao Yin

Subrata Chakrabarti

Michael W A Chu

Stephen M Sims

See next page for additional authors

Authors
Brittany Balint, Hao Yin, Subrata Chakrabarti, Michael W A Chu, Stephen M Sims, and J Geoffrey Pickering

Original Article

Collectivization of Vascular Smooth Muscle Cells via TGF-β–Cadherin-11–Dependent Adhesive Switching

Brittany Balint, Hao Yin, Subrata Chakrabarti, Michael W.A. Chu, Stephen M. Sims, J. Geoffrey Pickering

Objective—Smooth muscle cells (SMCs) in healthy arteries are arranged as a collective. However, in diseased arteries, SMCs commonly exist as individual cells, unconnected to each other. The purpose of this study was to elucidate the events that enable individualized SMCs to enter into a stable and interacting cell collective.

Approach and Results—Human SMCs stimulated to undergo programmed collectivization were tracked by time-lapse microscopy. We uncovered a switch in the behavior of contacting SMCs from semiautonomous motility to cell–cell adherence. Central to the cell-adherent phenotype was the formation of uniquely elongated adherens junctions, ≤60 μm in length, which appeared to strap adjacent SMCs to each other. Remarkably, these junctions contained both N-cadherin and cadherin-11. Ground-state depletion super-resolution microscopy revealed that these hybrid assemblies were comprised of 2 parallel nanotracks of each cadherin, separated by 50 nm. Blocking either N-cadherin or cadherin-11 inhibited collectivization. Cell–cell adhesion and adherens junction elongation were associated with reduced transforming growth factor-β signaling, and exogenous transforming growth factor-β1 suppressed junction elongation via the noncanonical p38 pathway. Imaging of fura-2–loaded SMCs revealed that SMC assemblies displayed coordinated calcium oscillations and cell–cell transmission of calcium waves which, together with increased connexin 43–containing junctions, depended on cadherin-11 and N-cadherin function.

Conclusions—SMCs can self-organize, structurally and functionally, via transforming growth factor-β–p38–dependent adhesive switching and a novel adherens junction architecture comprised of hybrid nanotracks of cadherin-11 and N-cadherin. The findings define a mechanism for the assembly of SMCs into networks, a process that may be relevant to the stability and function of blood vessels. **(*Arterioscler Thromb Vasc Biol*. 2015;35:00-00. DOI: 10.1161/ATVBAHA.115.305310.)**

Key Words: cadherin 5 ■ cell adhesion molecules ■ myocytes, smooth muscle

Cells within healthy tissues exist not as individual cells but as part of a collective. This paradigm of cell collectiveness is relevant to vascular smooth muscle cells (SMCs). SMCs within arteries directly associate with each other in layered, circumferential arrangements that provide structural integrity to the artery and enable it to constrict and relax in a coordinated manner.[1]

In contrast to healthy vessels, diseased arteries are characterized by disordered cellular arrangements.[2–5] For SMCs, this can entail residing outside of a cohesive network. For example, in atherosclerotic lesions, SMCs can exist as individual cells within an extracellular matrix, lacking critical connections to neighboring SMCs.[2,6] As well, in nonatherosclerotic but remodeling arteries, migrating and proliferating SMCs can have little association with neighbors.[4,7]

This dichotomy between individual and collective SMCs has implications for vascular health. In particular, the extent to which individual SMCs can successfully integrate into a functioning collective could be vital to imparting stability to the artery and enabling coordinated contractile activity. The latter depends on coordination of Ca^{2+} oscillations and waves among neighboring SMCs.[8] However, in contrast to the growing understanding of pathways that drive differentiation of SMCs,[9] relatively little is known about a transition from individual to collective SMCs. One reason for this is the paucity of in vitro models of SMC collectivization. In contrast to endothelial cells, which form a cohesive monolayer in culture, cultured SMCs form patterns that are less defined and less stable.

Central to the formation of cell collectives are the attachments cells make with each other. One important means by

Received on: July 18, 2014; final version accepted on: February 27, 2015.

From the Robarts Research Institute (B.B., H.Y., J.G.P.), Departments of Medicine (Cardiology) (J.G.P.), Biochemistry (J.G.P.), Medical Biophysics (B.B., J.G.P.), Pathology and Laboratory Medicine (S.C.), Surgery (M.W.A.C.), and Physiology and Pharmacology (S.C., S.M.S.), University of Western Ontario, London Health Sciences Centre (J.G.P.), London, Ontario, Canada.

The online-only Data Supplement is available with this article at http://atvb.ahajournals.org/lookup/suppl/doi:10.1161/ATVBAHA.115.305310/-/DC1.

Correspondence to J. Geoffrey Pickering, MD, PhD, London Health Sciences Centre, 339 Windermere Rd, London, Ontario N6A 5A5, Canada. E-mail gpickering@robarts.ca

Nonstandard Abbreviations and Acronyms	
SMC	smooth muscle cell
TGF-β	transforming growth factor-β

which cell–cell attachments are made is through adherens junctions, a specialized structure detected in almost all tissue-forming cells.[10] The major cell–cell adhesion receptors within adherens junction are cadherins, a group of transmembrane glycoproteins that mediate calcium-dependent homophilic adhesion, cell sorting, and tissue morphogenesis.[11] There is limited understanding of cadherins in vascular SMCs, although N-cadherin is believed to be the most abundant cadherin in SMCs.[12] This classical cadherin has been reported to regulate SMC proliferation,[13] SMC migration,[14] and the myogenic constrictor response.[12] Roles for other cadherins in SMCs are even less well studied. In addition, despite their importance in cell–cell adhesion, a role for cadherins in collective SMC decisions has not been determined.

Herein, we report a novel, adhesive switching phenomenon that drives SMC collectivization. Using human SMCs capable of undergoing programmed collectivization[15,16] and super-resolution microscopy, we establish that this adhesive switch entails the assembly of a previously unknown cadherin complex, comprised of hybrid nanotracks of cadherin-11 (osteoblast cadherin) and N-cadherin. We also demonstrate the centrality of cadherin-11 in both connecting SMCs to each other and in coordinating calcium oscillations and waves among SMCs.

Materials and Methods

Materials and Methods are available in the online-only Data Supplement.

Results

Induction of SMC Collectivization: Formation of Long-Duration Homotypic Cell Adhesions

To elucidate events that underlie SMC self-organization, we performed time-lapse video microscopy of HITC6 SMCs, a line of human SMCs that displays several physiological attributes[15,17] and undergoes programmed morphogenesis on serum withdrawal.[15,18] We specifically studied cells at low density to visualize the initial contact activity among SMCs. When cultured in medium supplemented with 10% fetal bovine serum, SMCs were seen to contact each other as they randomly migrated. However, the cell–cell associations were transient such that most cells remained individualized (Figure 1A, left). In contrast, on serum withdrawal, SMCs assembled into small collectives with end-to-end, end-to-side, and side-to-side cellular arrangements (Figure 1A, right).

Time-lapse assessment of contact dynamics for SMCs in serum-supplemented media revealed 2 dominant patterns. Most common was a profile of touch-and-release, whereby an approaching cell would extend all or part of a lamellipod toward a neighboring cell, make contact, and then break contact and continue migrating (Figure 1B; Video I in the online-only Data Supplement). A second pattern entailed an approaching cell making contact with a neighbor but then effectively sliding over or under its surface, traversing to the opposite side of the cell (Figure 1C; Video I in the online-only Data Supplement). In contrast to these profiles, contacts among SMCs in serum-free media were followed by consolidation of the cell–cell attachments. In some instances, this involved additional contact sites between the 2 cells and progressive coalignment to form a SMC bundle, similar to that present in vivo (Figure 1D; Video II in the online-only Data Supplement). In other instances, there was spreading of the contact interface, sometimes despite tugging between contacting but motile cells, suggesting strengthened cell–cell adhesions. As well, additional contacts could be made with other cells, which generated a multicellular network (Figure 1E; Video III in the online-only Data Supplement).

Quantitative analysis confirmed these distinctions between the 2 culture conditions. For SMCs in serum-supplemented media, the median contact duration was 2.4 hours (0.03–12 hours), whereas for cells under serum-free conditions, this was 9.3 hours (2.4–24 hours; $P<0.0001$; Figure 1F), a prolongation in contact duration that persisted after adjusting for SMC migration speed using multivariate analysis ($P<0.0001$). Based on the frequency distributions of contact duration (Figure 1F), we defined a long-duration adhesion as one that lasted >4.9 hours, corresponding to the 90th percentile of contact duration for SMCs in serum-supplemented media. Using this cut-point, 82% of contacts between SMCs under serum-free conditions progressed to long-duration adhesions (Figure 1F). In contrast, for SMCs under serum-supplemented conditions, only 10% of contacts evolved to long-duration adhesions. Instead, these cells displayed an increased propensity for touch-and-release behavior (7.8-fold; $P<0.0001$) and cell traversing (3.0-fold; $P=0.0048$; Figure 1G). We also determined that the serum withdrawal–induced shift to an adhesive SMC phenotype was relatively rapid, with 63±4% of all cells entering into a collective (long-duration adhesions) doing so within 4 hours (Figure 1H). Increased contact duration after serum withdrawal was also observed for human coronary SMCs and human dermal fibroblasts (Figure I in the online-only Data Supplement).

Collectively, these time-lapse contact data establish that SMCs can switch from a noncell-adhesive phenotype to a cell-adhesive phenotype. This shift is characterized by the acquisition of a repertoire of postcontact behavior patterns that drive cell collectivization and that are distinct from the contact behavior that enables individual cell motility.

SMC Collectivization Is Characterized by the Formation of Strikingly Elongated Adherens Junctions

To elucidate the adhesive machinery underlying SMC collectivization, we imaged cell–cell interfaces by transmission electron microcopy. This revealed the presence of electron-dense zones at interfaces consistent with adherens junctions. These measured 348±29 nm in length and were found in both serum-supplemented SMC cultures and in cultures studied 5 hours after serum withdrawal. However, under serum-supplemented conditions, partial or asymmetrical electron densities

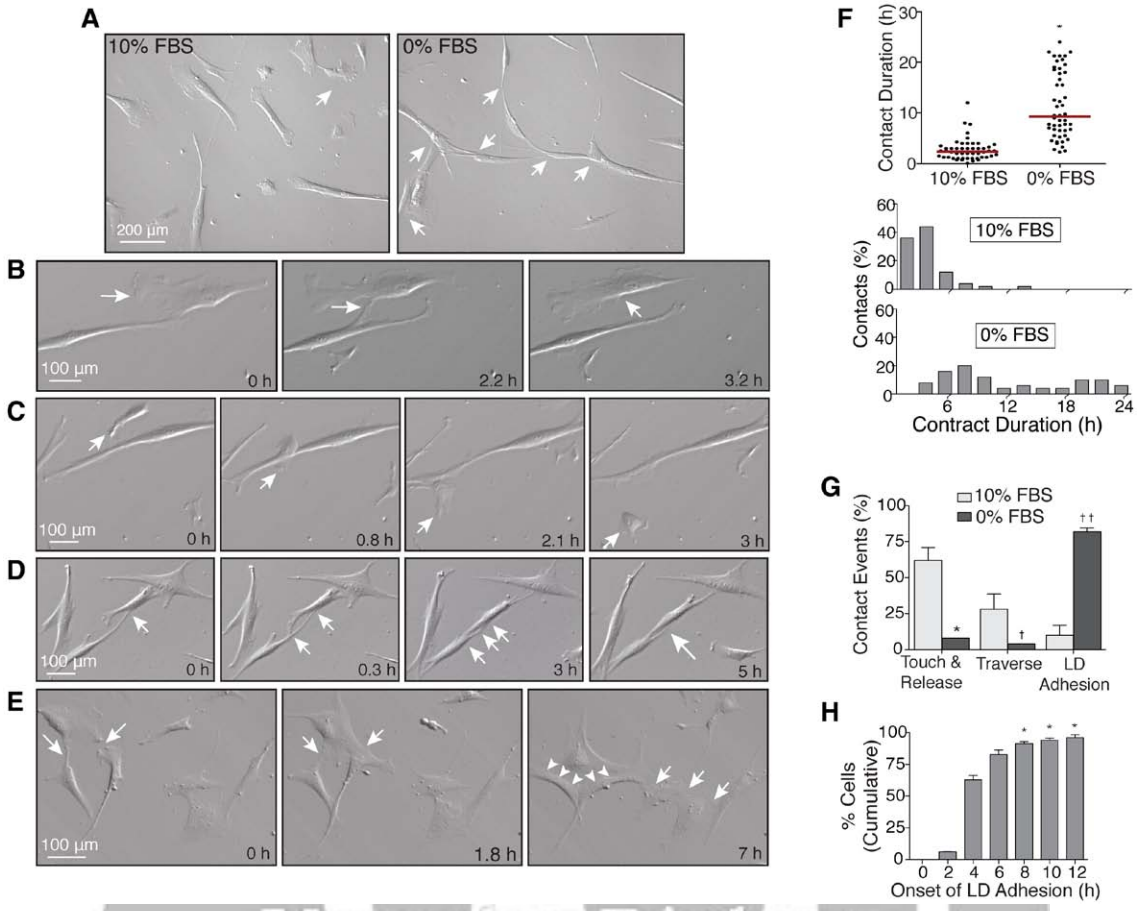

Figure 1. Smooth muscle cells (SMCs) can be induced to switch from individual to collective behavior. **A**, Photomicrographs of HITC6 SMCs in media supplemented with 10% fetal bovine serum (FBS; **left**) and 12 hours after serum withdrawal (**right**) showing network formation at low density. Arrows depict intercellular contacts. **B**–**E**, Still-frames from time-lapse images of HITC6 SMCs illustrating touch-and-release (**B**) and cell traversing (**C**) behavior for SMCs in 10% FBS and stabilized cell–cell contacts for SMCs in 0% FBS (**D** and **E**). The arrows in **B** depict a lamellipod site before, during, and after contact with the adjacent cell. Arrows in **C** indicate a SMC as it contacts and then translocates over another cell. Arrows in **D** show the accumulation of side-by-side SMC attachments. Arrows in **E** depict the contacts among SMCs forming a concatenated network. The arrowheads depict spreading of a contact interface. Corresponding videos for **B**–**E** are available in the online-only Data Supplement. **F**, Graph depicting median contact time between SMCs in media supplemented with 10% FBS and after serum withdrawal (*P<0.0001). Frequency distributions of contact durations are shown below. **G**, Graph illustrating postcontact decision making, designated as touch-and-release, traverse, or long-duration (LD) adhesion (*P=0.0440, †P=0.0002, and ††P<0.0001). **H**, Graph illustrating the onset of LD adhesions after serum withdrawal (*P<0.0001).

were observed, suggesting junctions that had either failed to completely assemble or were in the process of disassembling. Adherens junctions between SMCs under serum-free conditions were consistently symmetrical, with no evidence for partial assembly (Figure 2A).

We next evaluated the morphology of adherens junctions in SMCs by immunostaining for cadherins, using a pan-cadherin antibody. This revealed abundant linear aggregates of cadherins in a ladder-like formation along the interfaces of contacting SMCs (Figure 2A, bottom left). These were closely associated with the ends of microfilament bundles. However, there were pronounced differences in the lengths of the individual, linear cadherin clusters for the 2 culture conditions, with the median length for SMCs under serum-free conditions being 2.5-fold greater than that for SMCs under serum-supplemented conditions (P<0.0001). Furthermore, there was a relatively tight distribution of cadherin assembly lengths for SMCs under noncollectivizing conditions, whereas after serum withdrawal, the distribution was wider and prominently skewed to the right. This corresponded with the emergence of strikingly elongated assemblies that reached ≤59.8 μm in length (versus 19.2 μm for SMCs in 10% fetal bovine serum; Figure 2A bottom right; Figure 2B). These unusual linear assemblies gave the appearance of cells being strapped together.

Immunostaining SMCs for β-catenin showed a similar elongation response after serum withdrawal, with pronounced β-catenin clusters that ran parallel to actin microfilament bundles at cell–cell contacts. In contrast, immunostaining for pFAK showed typical focal adhesion clustering, with no evidence for elongation of signal on serum withdrawal (Figure II in the online-only Data Supplement).

Cadherin-11 Mediates SMC Collectivization

Over 100 members of the cadherin family have been sequenced. To gain an unbiased view of specific cadherins that might mediate SMC collectivization, we interrogated microarray expression data from HITC6 SMCs (GEO GSE21363). Using a signal intensity cut-point of twice that

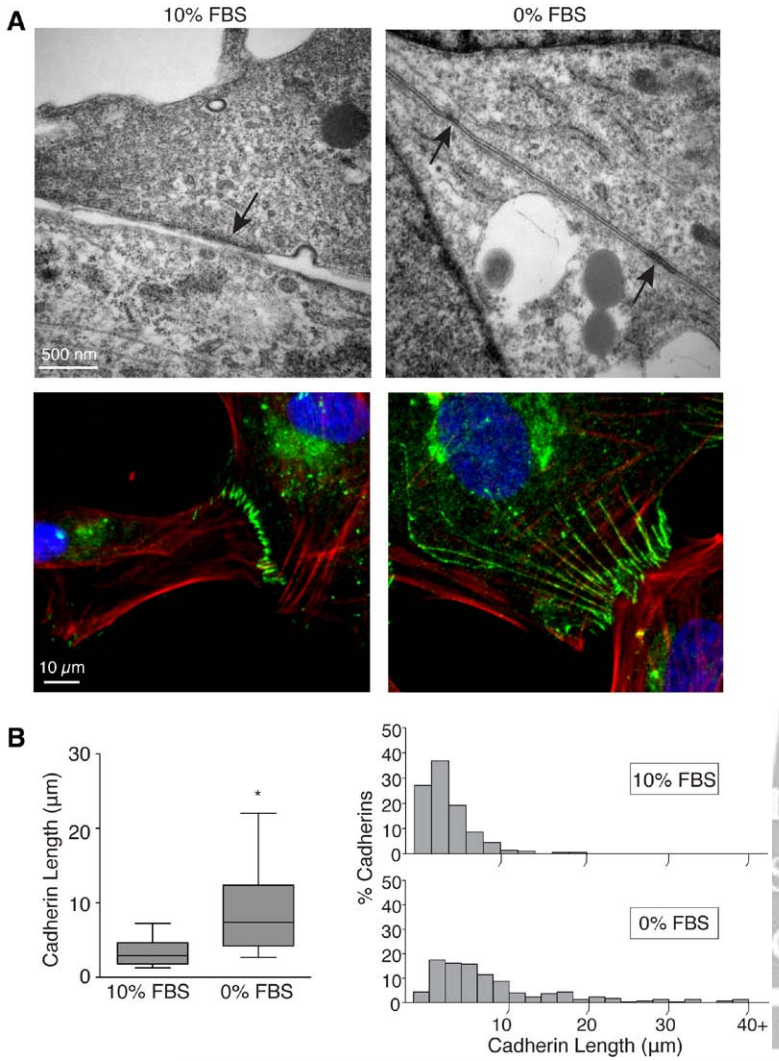

Figure 2. Adherens junctions are symmetrical and elongated between collectivized smooth muscle cells (SMCs). **A**, **Top**, Electron micrographs of SMCs in medium with fetal bovine serum (FBS), showing adherens junctions with asymmetrical electron densities, and SMCs in medium without FBS, showing symmetrical adherens junctions (arrows). **A**, **Bottom**, Fluorescent micrographs of contacting SMCs immunostained with a pan-cadherin antibody and labeled with Texas-Red-X phalloidin and Hoechst 33258. For SMCs in 10% FBS (**left**), cadherins exist as short streaks near the ends of actin microfilament bundles. However, in serum-free media (**right**), cadherins are strikingly elongated. **B**, Box and whisker plot of median cadherin length, interquartile range, and 10th to 90th percentile range; n=358 and 297, cadherin aggregates for 10% and 0% FBS, respectively; **P*<0.0001. Corresponding frequency distributions are on the right and indicate a right-shift in cadherin length for cells in the absence of serum.

for the endothelial-specific vascular endothelial cadherin, we identified expression of 35 members of the cadherin superfamily in SMCs, including 13 cadherins, 20 protocadherins, and 2 flamingo-type cadherins (Table I in the online-only Data Supplement). Interestingly, none of these signals displayed significant increases in expression within 24 hours after serum withdrawal. Also interesting was that the strongest hybridization signal corresponded not to N-cadherin but to cadherin-11 (osteoblast cadherin), an atypical (type II) cadherin found on mesenchymal cells.[19,20] Western blot analysis confirmed the expression of cadherin-11 in SMCs and showed no change in expression of either cadherin-11 or N-cadherin ≤12 hours after serum withdrawal (Figure 3A).

Immunofluorescence microscopy revealed that cadherin-11 localized to adherens junctions between contacting SMCs, as did N-cadherin (Figure 3A). Moreover, on serum withdrawal, the median length of the linear cadherin-11 aggregates increased by 2.1-fold (*P*<0.0001) and that of N-cadherin increased by 1.5-fold (*P*<0.0001; Figure 3B). Elongation of cadherin assemblies was likewise observed in coronary artery SMCs after serum withdrawal (Figure III in the online-only Data Supplement). Thus, both type I and type II cadherins participated in the dynamic remodeling of adherens junctions during SMC collectivization.

To further assess causality, we performed live-cell imaging in the presence of blocking antibodies or IgG control. When applied to serum-free and otherwise collectivizing SMC cultures, the cadherin-11 blocking antibody, AF1790, led to a 74% decline in the median SMC–SMC contact duration (*P*<0.0001), a 60% decline in the proportion of long-duration contact events (*P*<0.0001), and a 3.5-fold increase in the proportion of touch-and-release contact events (*P*=0.001; Figure 3C). Interestingly, blockade of N-cadherin, using antibody GC-4, also reduced the cell–cell contact duration (*P*<0.0001) and increased touch-and-release behavior (*P*=0.0025; Figure 3D). Specificity of both blocking antibodies was confirmed by immunostaining SMCs incubated with the blocking antibody for the homologous and heterologous cadherins (Figure IV in the online-only Data Supplement). As well, inhibiting the expression of cadherin-11 or N-cadherin with siRNA led to reduced SMC contact duration, with incrementally suppressed cell adhesion on knocking down expression of both cadherins (Figure V in the online-only Data Supplement).

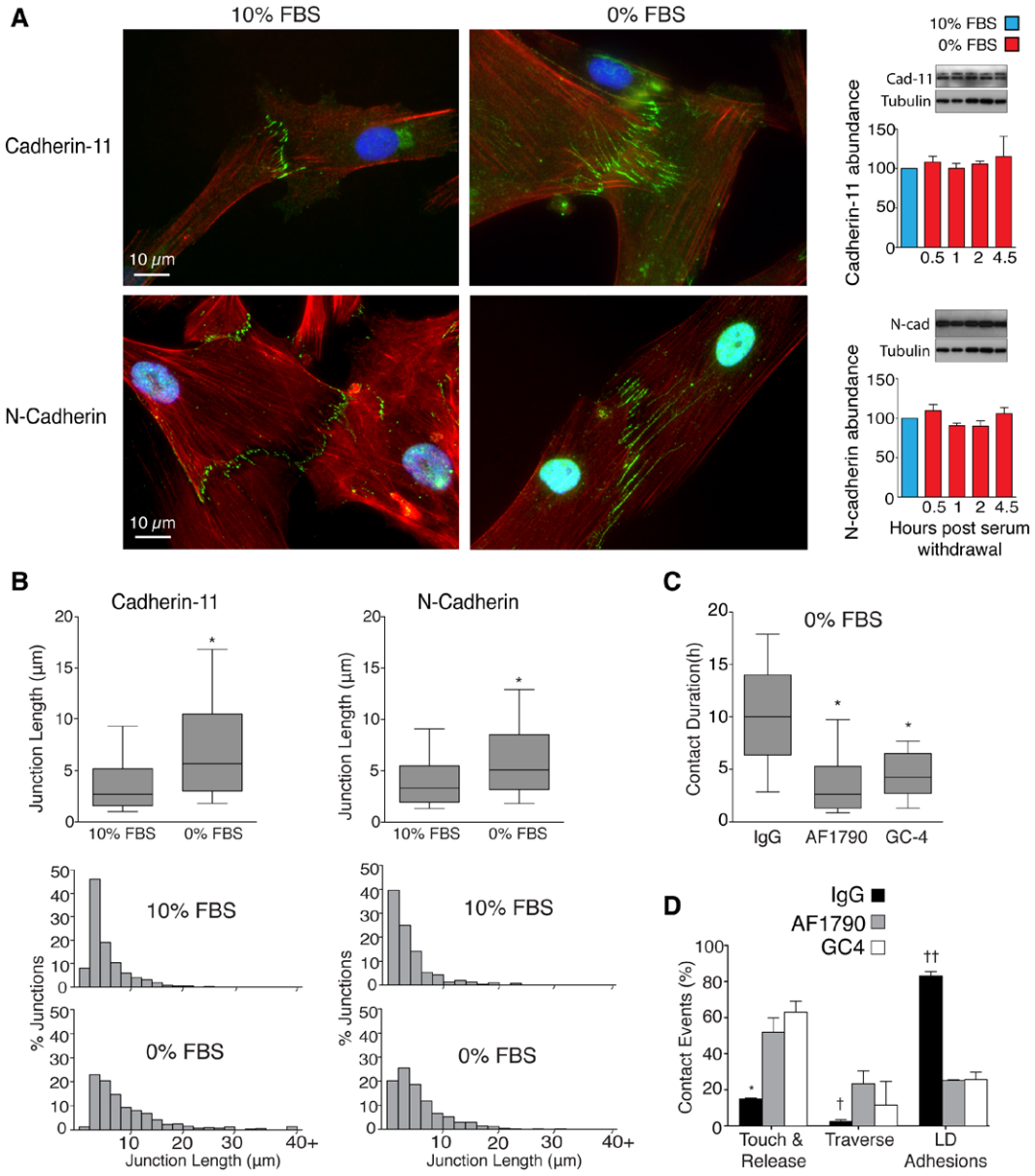

Figure 3. Cadherin-11 and N-cadherin are expressed in smooth muscle cells (SMCs) and mediate collective SMC behavior. **A**, Fluorescent micrographs of HITC6 SMCs in serum-supplemented (**left**) and serum-free medium (**right**) stained for cadherin-11 (**top**) and N-cadherin (**bottom**) and counterstained with Texas-Red-X phalloidin and Hoechst 33258. Western blots and quantification depicting stable expression of cadherin-11 (P=0.90) and N-cadherin (P=0.48). **B**, Box and whisker plots depicting median cadherin length before and after (n=569; n=486) serum withdrawal, with corresponding frequency distributions of cadherin lengths depicted below; *P<0.0001. **C**, Graph depicting the effect of blocking antibodies against N-cadherin (GC-4), cadherin-11 (AF1790), or control IgG on cell–cell contact duration for SMCs under serum-free, collectivizing conditions; *P<0.0001. **D**, Graph depicting the effect of cadherin-11 or N-cadherin blockade on postcontact decisions between SMCs under serum-free, collectivizing conditions. *P=0.0010 vs AF1790, P=0.0025 vs GC-4; †P=0.0003 vs AF1790, P=0.0152 vs GC-4, ††P=0.0005 vs AF1790, and P=0.0018 vs GC-4.

Super-Resolution Microscopy Reveals Hybrid Nanotrack Assemblies of Cadherin-11 and N-Cadherin

To better understand the relationship between cadherin-11 and N-cadherin in SMCs, we assessed their relative locations by double immunolabeling. Remarkably, this revealed an unexpected pattern of coassembly of both cadherin types present within a given linear adherens junction aggregate. However, we also noted that the colocalization was partial with discrete regions of cadherin-11 and N-cadherin along the length of the junctional straps (Figure 4A).

To further delineate this spatial relationship, we undertook super-resolution imaging using ground-state depletion microscopy. Interestingly, this revealed that the 2 cadherins were in fact resolvable at the nanoscale level. Surprisingly, the cadherins assembled into 2 parallel tracks, one for each cadherin, which were separated by 51±5 nm (Figure 4B). These paired nanotracks constituted the adherens junction assemblies for SMCs under both serum-supplemented and serum-free conditions and have never been described before to our knowledge. Moreover, because the 2 cadherins were distinguishable, we were able to quantify their relative proportions in the paired-track assemblies,

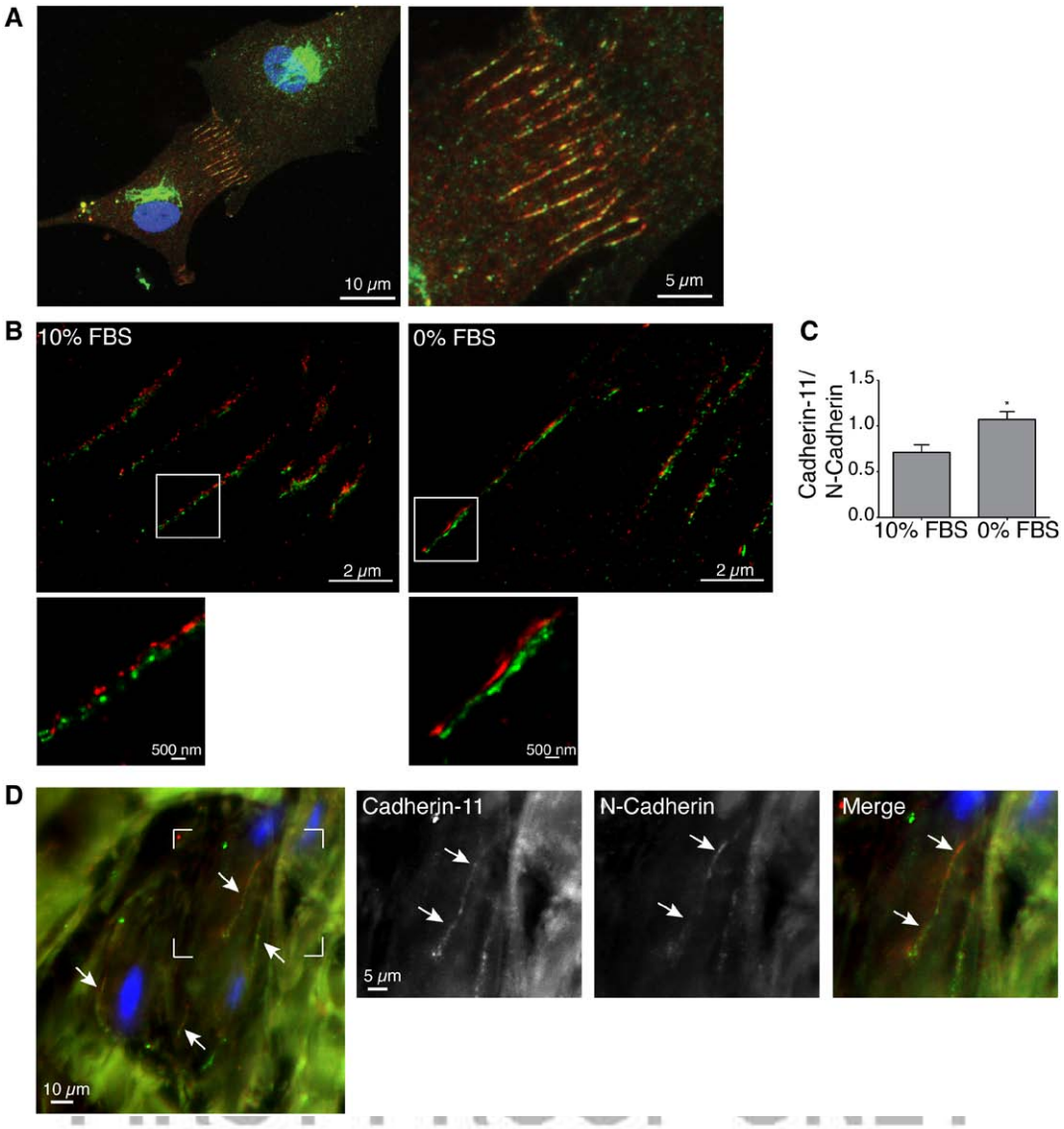

Figure 4. Cadherin-11 and N-cadherin coexist in adherens junctions as parallel nanotracks. **A**, Wide-field fluorescent microscopy image of contacting smooth muscle cells (SMCs) double-immunolabeled for cadherin-11 (green) and N-cadherin (red) showing coexistence of the 2 cadherins within a given immunodectable junction. **B**, Ground-state depletion super-resolution microscopy images showing physical separation of cadherin-11 from N-cadherin as parallel nanotracks within a given linear junction aggregate for SMCs under both serum-supplemented and serum-free conditions. Zoomed regions of the areas within the white boxes are shown. **C**, Graph depicting the ratios of the area of cadherin-11 to that of N-cadherin, within a given linear junction aggregate, before (n=34) and 5 hours after (n=35) serum withdrawal, showing relative enrichment of cadherin-11; **P*=0.0039. **D**, Fluorescent micrographs of a tangential section of the media of the thoracic ascending aorta immunostained for cadherin-11 (green), N-cadherin (red), and nuclei (Hoechst 33258, blue). Linear aggregates of both cadherins can be seen between adjacent cells (arrows). Region within the box corners are depicted in the second row.

based on area fractions. This revealed that 5 hours after serum withdrawal, there was a 1.5-fold increase in the proportion of cadherin-11 in the complex (*P*=0.0012), indicating the enrichment of cadherin-11 under collectivizing conditions (Figure 4C).

Hybrid Cadherin-11/N-Cadherin Assemblies Are Present in the Media of the Human Thoracic Aorta

To determine whether the unique adherens junction attributes we identified in collectivizing SMCs reflected an in vivo phenomenon, we immunostained sections of human thoracic aorta retrieved at the time of heart transplantation. To optimize identifying contacts between SMCs, the aortic specimens were tangentially sectioned through the media and double-immunolabeled for cadherin-11 and N-cadherin. This revealed discrete, elongated adherens junctions between cells that spanned ≤30 μm in length. Moreover, both cadherin-11 and N-cadherin could be identified within a given linear aggregate. The 2 cadherins appeared intimately associated but, similar to the findings in vitro, signal overlap was not absolute suggesting some separation (Figure 4D).

SMC Collectivization and Assembly of Adherens Strap–Like Junctions Depend on Withdrawal of Transforming Growth Factor-β Signaling

The time course of SMC collectivization after serum withdrawal indicated that acquisition of a strongly adhesive SMC

phenotype was both rapid and regulatable. Transforming growth factor (TGF)-β1 is a major component of serum[21] and a factor that promotes SMC–extracellular matrix attachments.[22] We, therefore, next asked whether the propensity for SMC networking and associated adherens junction dynamics were regulated by TGF-β signaling. Interestingly, withdrawal of serum from SMC cultures led to a 49% decline in the abundance of phosphorylated SMAD2 (Ser465/467) within 2 hours, indicating that reduced TGF-β signaling accompanied the initiation of the adhesive switch (Figure 5A; P=0.0218). Consistent with this, addition of recombinant TGF-β1 to serum-free SMCs caused a 68% reduction in cell–cell contact duration (P<0.0001; Figure 5B), and conversely, si-RNA–mediated knockdown of the TGF-β receptor-1 increased the contact duration for SMCs in serum-supplemented media (Figure 5B). Exogenous TGF-β1 also yielded a 62% decrease in the proportion of long-duration contacts (P=0.0187; Figure 3C) and a 24.6-fold increase in the proportion of contacting SMCs that exhibited touch-and-release behavior (P=0.0002; Figure 5C).

This TGF-β–driven shift in cell–cell contact dynamics was associated with concordant effects on the morphology of cadherin assemblies. Electron microscopy revealed that incubation with TGF-β1 for 5 hours affected the normally symmetrical adherens junctions in SMCs under serum-free conditions, such that hemijunctions were again visible (Figure 5D). As well, TGF-β1 abrogated the serum withdrawal–induced elongation and rightward skewing of the length distribution of cadherin-11/N-cadherin–containing adherens junctions (median, 5.7 versus 2.9 μm and 5.1 versus 2.8 μm; P<0.0001 for both; Figure 5D). Abrogation of cadherin-11 elongation by TGF-β1 was also observed for SMCs in confluent cultures (Figure VI in the online-only Data Supplement). Thus, the rapid conversion of SMCs to a cell adhesive, collectivizing phenotype depends on blunting of TGF-β signaling.

To elucidate the signaling arm downstream of TGF-β responsible for controlling the cadherin assemblies, TGF-β1–stimulated SMCs were incubated with selective signaling inhibitors. Interestingly, inhibiting TGF-β receptor-1 kinase

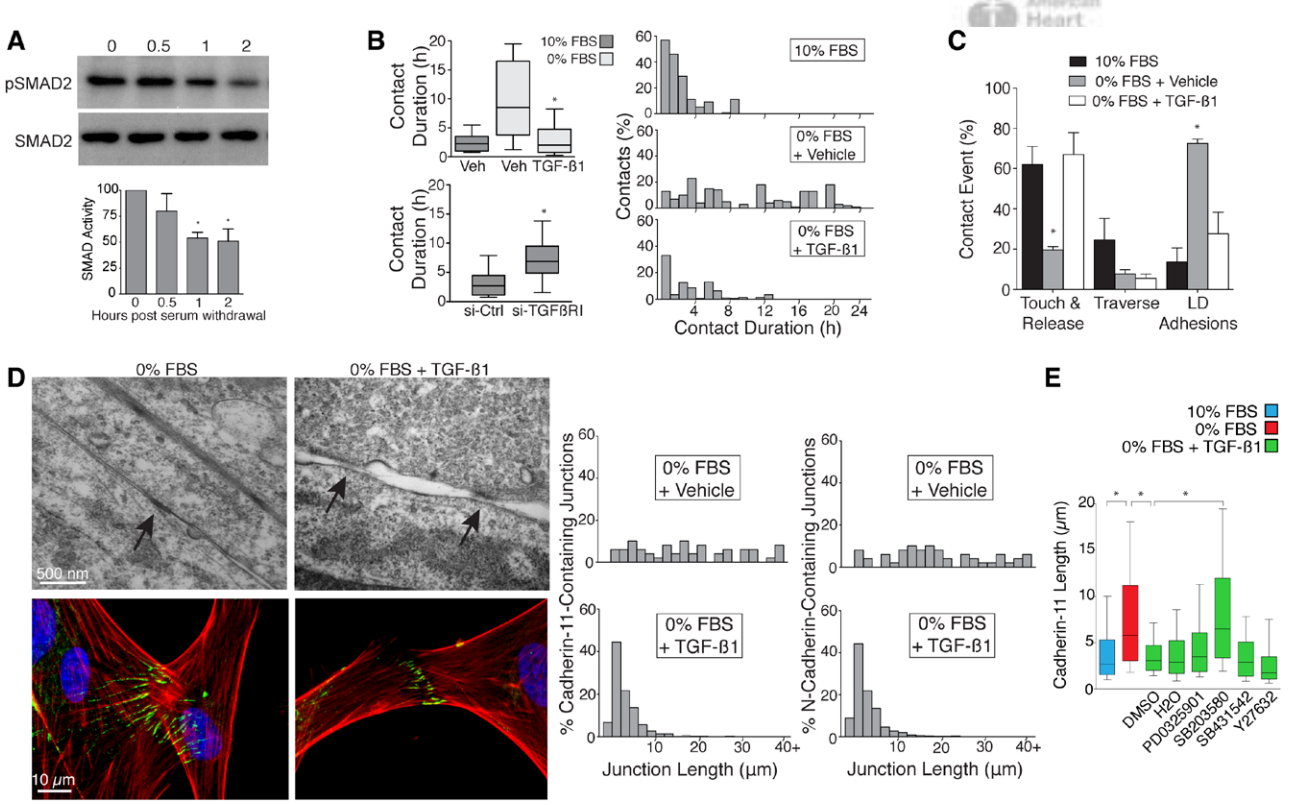

Figure 5. Attenuation of transforming growth factor-β (TGF-β) signaling is required for smooth muscle cell (SMC) collectivization. **A**, Western blot showing a decline in abundance of phosphorylated SMAD2 within 1 hour of serum withdrawal. Densitometry data are depicted below the blots (*P=0.0218; n=3). **B**, Box and whisker plots depicting a decrease in the median cell contact duration on addition of TGF-β1 (10 ng/mL) to SMCs under serum-free, collectivizing conditions (*P<0.0001) and an increase in contact duration in 10% fetal bovine serum (FBS)–supplemented media when TGF-β signaling is blocked using TGF-βR1 siRNA (*P<0.0001). The corresponding frequency distributions of contact durations are shown on the right, illustrating a TGF-β1–induced abrogation of the right-shifted distribution. **C**, Graph depicting the influence of TGF-β1 on postcontact decision making between contacting SMCs (touch-and-release: P=0.0008 vs TGF-β1, traverse: P=0.963 vs TGF-β1; long-duration (LD) adhesions: P=0.0068 vs TGF-β1). **D**, **Top**, Electron micrographs of SMCs in media without serum, with (**left**) and without (**right**) TGF-β1. A well-developed, symmetrical adherens junction between adjacent cells is evident under control conditions (arrow), whereas under TGF-β1–stimulated conditions unilateral junction electron densities were present (arrows). **D**, **Bottom**, Fluorescent micrographs of SMCs under serum-free, collectivizing conditions immunostained using a pan-cadherin antibody showing abrogation of the highly elongated adherens junction aggregates by TGF-β1. **D**, **Right**, Graphs depicting cadherin-11 and N-cadherin junction length distributions in SMCs in media with 0% FBS, with or without TGF-β1, showing a left-shift of the distribution for both cadherin-11 and N-cadherin–containing junctions in the presence of TGF-β1. **E**, Box and whisker plot depicting the effect of TGF-β pathway blockers on the length of cadherin-11 assemblies. Blocking p38 signaling, but not SMAD2/3, extracellular signal–regulated kinases 1/2, or Rho kinase signaling, reversed TGF-β–induced shortening of adherens junctions (*P<0.0001).

activity with SB431542 did not block the effect of TGF-β1 on adherens junction length nor did inhibit extracellular signal–regulated kinases 1/2 or Rho kinase activity. However, inhibition of p38 kinase with SB203580 abrogated the TGF-β1–induced adherens junction shrinkage (median junction length, 6.50 versus 3.09 μm; $P<0.0001$; Figure 5E).

Cadherin-11–Dependent Collectivization Coordinates Calcium Transients Among SMCs

We next sought to determine whether cadherin-mediated collectivization enabled communication among SMCs in addition to the mechanical cohesion. To address this, we investigated patterns of $[Ca^{2+}]_i$ transients. SMCs were loaded with the Ca^{2+} indicator fura-2 and changes in fluorescence ratio were tracked for 5 to 15 minutes. SMCs were studied at low density, similar to that used to assess contact dynamics. Under these conditions, spontaneous and periodic calcium oscillations were found in 78.6±4.3% of SMCs in serum-supplemented media and 85.3±6.9% of SMCs in serum-free media. Among SMCs with $[Ca^{2+}]_i$ oscillations, the mean oscillation frequency was 3.84±0.66 (n=85) transients per minute for SMCs in serum-supplemented media and 3.80±0.64 transients per minute for cells in media with no serum (n=61; $P=0.963$).

Despite these similarities in basal frequency, different patterns of $[Ca^{2+}]_i$ transients were apparent. To determine whether there was coordination of $[Ca^{2+}]_i$ transients among contacting SMCs, we quantified the proportion of coincident $[Ca^{2+}]_i$ transients, correcting for the background proportion of coincident transients among noncontacting SMCs in the same dish. Assessment of the $[Ca^{2+}]_i$ transient time-plots revealed 2 patterns of $[Ca^{2+}]_i$ oscillations: independent and coordinated. Coordinated oscillations between contacting SMCs were prevalent under serum-deprived conditions and included phase-locked oscillations (Figure 6A). Overall, there was a 3.2-fold increase in the percentage of coincident $[Ca^{2+}]_i$ transients for contacting SMCs in serum-free media compared with serum-exposed SMCs ($P=0.0010$; Figure 6B). To investigate whether coordination of $[Ca^{2+}]_i$ transients was mediated by cadherin-11, SMCs subjected to serum withdrawal were incubated with the blocking antibody AF1790 or control IgG. Blocking cadherin-11 yielded a 47% decline in the prevalence of coincident Ca^{2+} transients among contacting SMCs ($P=0.0428$; Figure 6D). This entailed a 41% reduction in the prevalence of overlapping but nonphase-locked transients ($P=0.0163$) and complete abrogation of phase-locked synchrony ($P=0.013$). Blocking N-cadherin also significantly reduced the prevalence of coincident calcium transients ($P=0.037$) and abrogated phase-locked synchrony ($P=0.035$; Figure 6D).

Notably, the spontaneous $[Ca^{2+}]_i$ transients commonly appeared as waves. In some instances, these waves were seen to propagate from one cell to an adjacent cell. Such waves were transmitted at the cell–cell contacts site, with only a modest time delay in propagation across the contact site (Figure 6C and Videos IV and V in the online-only Data Supplement). This phenomenon constituted 21% of coordinated transients among contacting SMCs under serum-deprived conditions but was not observed in any of the transients among contacting cells under serum-supplemented conditions ($P=0.0096$) nor in any of the transients in SMCs subjected to either cadherin-11 or N-cadherin blockade ($P=0.011$ and $P=0.035$, respectively).

To determine whether this feature of SMC collectivization was associated with gap junctions, we immunostained cells for the gap junction protein, connexin 43. This revealed connexin 43 clusters at SMC–SMC contact sites, aggregates that were commonly associated with the ends of actin microfilament bundles (Figure 6E). The proportion of contacting SMC pairs in which gap junction aggregates were identified was significantly higher under serum-free, collectivizing conditions (78.6±5.5 versus 36.5±6.2%; $P=0.0001$). Furthermore, antibody-mediated blockade of cadherin-11, N-cadherin, or both reduced the proportion of SMC–SMC pairs with immunodetectable connexin 43 clusters by 62%, 47%, and 70%, respectively ($P=0.0007$, $P=0.0006$, and $P<0.0001$, respectively; Figure 6F).

Taken together, these findings establish that reinforcement of SMC–SMC cohesion, through the combined actions of cadherin-11 and N-cadherin, leads to coordinated $[Ca^{2+}]_i$ oscillations and wave propagation among SMCs, pointing to functional connectivity.

Discussion

In diseased arteries, SMCs can reside as individual cells, but in healthy arteries, they exist as highly ordered collectives. The findings herein identify a paradigm by which a shift from individual to collective SMCs can occur. Notably, collectivization of adult SMCs was not determined by the proximity of SMCs to each other but, instead, by the acquisition of a distinct SMC-adherent phenotype. The shift to this adherent phenotype required blunting of TGF-β signaling and yielded SMCs that formed strikingly elongated adherens junctions when they contacted an adjacent SMC. Remarkably, these adherens junctions were hybrids of N-cadherin and cadherin-11, organized as parallel nanotracks of each cadherin. This previously unknown cadherin formation served not only to hold SMCs together but also to coordinate calcium transients among connected SMCs. These findings define a mechanism for self-assembly of SMCs into integrated units.

Time-lapse microscopy revealed that SMCs with a nonadherent phenotype effectively ignored each other on contact or, at most, formed transient contacts. In contrast, SMCs with a cell-adherent phenotype developed long-duration connections and self-organized into collectives. This cadherin-mediated shift from nonsocial to social behavior was notable for its rapidity, becoming evident between 2 and 4 hours after serum withdrawal. This time course, together with the stable expression of cadherin-11 and N-cadherin during this time frame, suggests that reconfiguring existing adhesion machinery is a powerful means of driving SMC cohesion. The potential for cadherin-11 and N-cadherin–based cohesion machinery to operate in vivo was supported by expression of these cadherins at SMC junctions in the human aorta. Moreover, the findings are in keeping with previously established paradigms of cadherin-based cell clustering during development, such as during somite formation.[23,24]

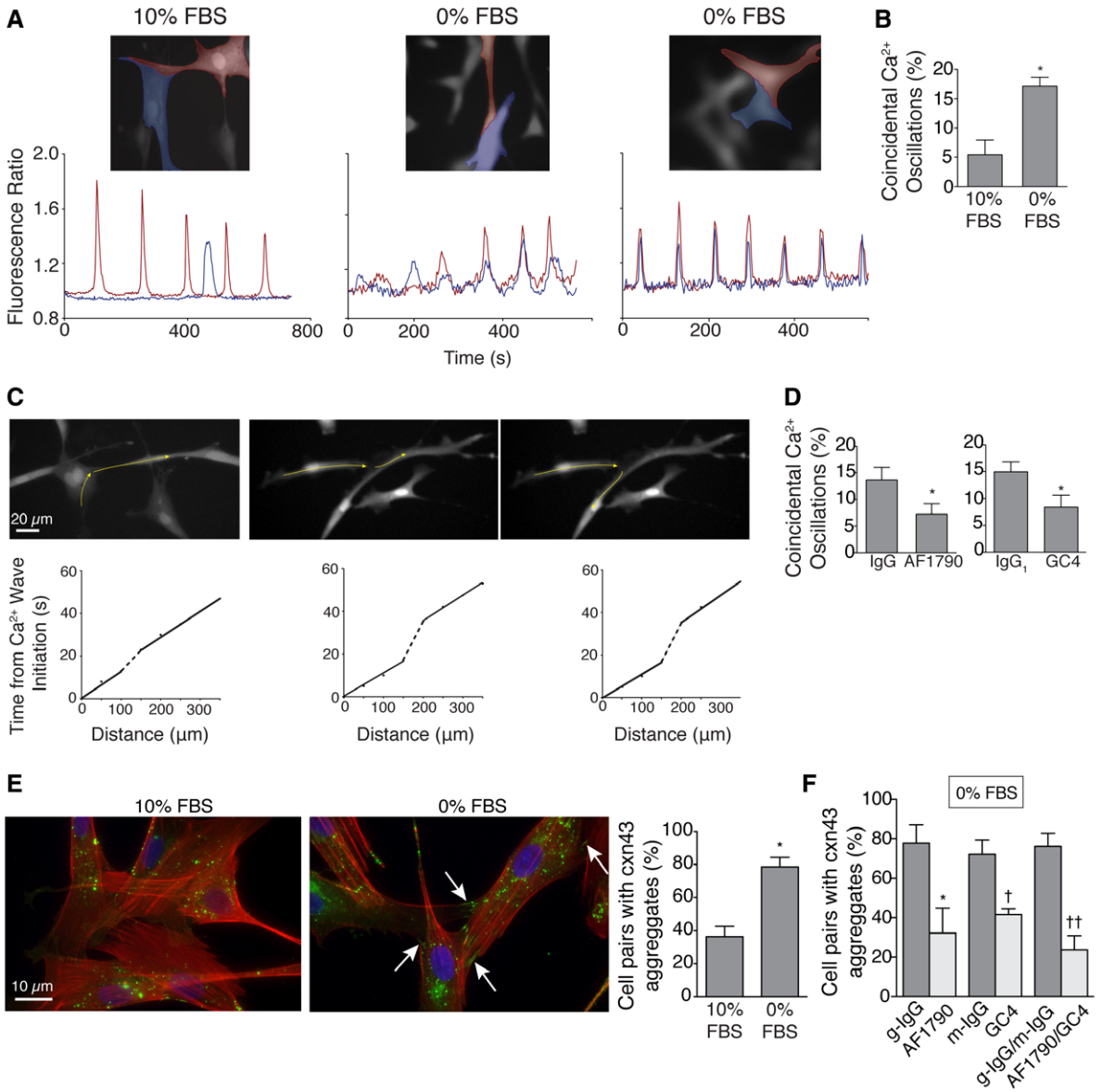

Figure 6. Calcium transients are coordinated among cadherin-11–dependent collectivized smooth muscle cells (SMCs). **A**, Spontaneous $[Ca^{2+}]_i$ oscillations in contacting SMCs cultured in the presence of 10% fetal bovine serum (FBS; noncollectivizing, short-duration adhesions) or 0% FBS (collectivizing, long-duration adhesions). Fluorescence ratios of fura-2–loaded SMCs are expressed relative to their respective baseline ratios at the start of the recording period and are plotted over time. Signals depicted are from the corresponding color-shaded cells in the fluorescent micrographs (images from 380-nm excitation). In FBS-supplemented media, independent oscillations are evident. **Middle** (0% FBS), Partial synchrony among the SMCs is seen. **Right** (0% FBS), SMCs display phase-locked synchrony of Ca^{2+} oscillations. **B**, Graph depicting the proportion of coincidental $[Ca^{2+}]_i$ oscillations among contacting SMCs in the presence or absence of FBS; **P*=0.0010. **C**, Fluorescent micrographs of contacting SMCs in 0% FBS that display propagation of $[Ca^{2+}]_i$ waves. The wave pathways are depicted by the yellow arrows and in the corresponding video files (Videos IV and V in the online-only Data Supplement). Graphs below each micrograph chart depict the timing of the wavefront at a given location, establishing that the wave begins in the downstream SMC at the cell–cell contact site. **D**, Graphs depicting the influence of cadherin-11–blocking antibody, AF1790, and N-cadherin–blocking antibody, GC-4, on the percentage of coincident $[Ca^{2+}]_i$ transients between contacting SMCs under collectivizing culture conditions; **P*=0.0428 and 0.037, respectively. **E**, Fluorescent micrographs of contacting SMCs and corresponding quantification of cell pairs with connexin 43 aggregates. Arrows indicate connexin 43 assemblies at cell–cell junctions (**P*=0.0001). **F**, Graph depicting the effect of cadherin–blocking antibodies or respective control mouse (m) or goat (g) IgG on the proportion of cell pairs with connexin 43 aggregates (**P*=0.0006, †*P*=0.0007, and ††*P*<0.0001 vs respective control IgG, ††*P*=0.049 vs SMCs incubated with GC-4).

Cadherins are known to assemble into different morphologies in different cell types.[10] However, the strikingly elongated adherens junctions, ≤60 μm in length, in collectivizing SMCs constitute a morphological profile not reported previously to our knowledge. N-cadherin has been identified in both punctate and linear morphologies in SMCs,[25,26] but functional correlates have not been established. Previous studies have determined that clustering of cadherins is a means of increasing adhesive strength, presumably by accumulating and concentrating cadherin bonds.[27] In light of the strap-like assemblies of cadherins in collectivizing SMCs and the abrogation of collectivization by cadherin blocking or expression

knockdown, we propose that cadherin-11/N-cadherin cluster length in SMCs is a key determinant of adhesive versus individualized SMC behavior.

The relative abundance of cadherin-11 in SMCs was surprising, given that N-cadherin is regarded as the major cell–cell adhesion molecule in vascular SMCs.[12] Although there is limited information on atypical cadherins in vascular cells, cadherin-11 has been reported to be upregulated in SMCs in vein grafts[28] and required for in vitro differentiation of mesenchymal stem cells to SMCs.[29] The current findings are the first to establish a role for cadherin-11 in structural networking among SMCs. Recent adhesion force measurements by Hinz et al[30] have established that cadherin-11 bonds are stronger than those of N-cadherin. This is noteworthy in light of our finding of enrichment of cadherin-11 at adherens junctions not only through junction elongation but also relative to N-cadherin. These findings suggest that differential cadherin composition at junctions could underlie differences in the stability of SMC networks.

SMC collectivization and adherens junction reinforcement were suppressed by TGF-β1 and mimicked by knocking down expression of TGF-β receptor-1. Although TGF-β may not be the only regulator of cell adhesion dynamics, these findings add to the repertoire of TGF-β actions on vascular SMCs. In this regard, it is noteworthy that TGF-β stimulates the differentiation of SMCs.[9] From a developmental standpoint, differentiation of SMCs from precursors would be expected to precede the development of firm SMC–SMC adhesions. The current findings thus suggest that tempering of TGF-β signaling may be required for a post-SMC differentiation phase of collectivization and assembly. It is also well recognized that TGF-β stimulates extracellular matrix production[31] and consolidates focal adhesions to the extracellular matrix.[22] This raises the possibility that withdrawal of TGF-β signaling might promote a shift from SMC–matrix interactions, which are dominant for individualized SMCs, to SMC–SMC interactions, which are required for SMC collectivization. Also noteworthy was that, although reduced TGF-β signaling was indicated by reduced Smad2 activity, it was the noncanonical, p38-dependent TGF-β cascade that regulated adherens junction length. Although further studies are required to better place the diverse actions of TGF-β in context, the current findings indicate that tuning of the TGF-β signaling environment may be a key determinant of individual versus collective decision making.

Using super-resolution ground-state depletion microscopy, we identified a cadherin nanoarchitecture within an adherens junction that has not been revealed before. The hybrid assemblies identified were comprised of 2 parallel cadherin tracks, one for N-cadherin and one for cadherin-11, separated by ≈50 nm. Interestingly, the observed separation between the 2 tracks implies that the arrangement does not contravene the paradigm of homophilic cadherin–cadherin binding or homotypic lateral clustering of cadherins.[10] Although both cadherin-11 and N-cadherin appeared to be within a given linear adherens junction assembly, they were in separate microdomains. The reason for the paired nanotrack architecture is unknown at this point and warrants investigation, including defining the mechanisms for cadherin sorting and targeting. However, we speculate that the additional complexity afforded by the track architecture could underlie a novel mechanism for regulating the force of adhesions. Moreover, the potential for this complexity to be relevant to the vessel wall was supported by our finding of hybrid cadherin-11/N-cadherin assemblies between medial SMCs in the human thoracic aorta.

A key reason for an interconnected arterial SMC network is to coordinate calcium signaling to enable productive arterial vasomotion. It was noteworthy, therefore, that within 5 hours of initiating SMC collectivization, we observed coordinated spontaneous $[Ca^{2+}]_i$ transients among contacting SMCs. This included more homogeneous $[Ca^{2+}]_i$ oscillation frequencies and, in some instances, phase-locked synchrony of $[Ca^{2+}]_I$ transients, changes that were dependent on cadherin-11 function. Particularly, noteworthy was the propagation of $[Ca^{2+}]_i$ waves from one cell to an adjacent contacting cell. Adherens junctions are not known to be conduits for Ca^{2+} movement, and at least 2 possibilities exist to explain the observed $[Ca^{2+}]_i$ wave propagation. First, the calcium coupling may be based on cell–cell transmission of mechanical forces, via the consolidated adherens junctions. This was suggested by the brief time delay between the end of a $[Ca^{2+}]_i$ wave in one cell and initiation in the second. Although we did not measure mechanical forces, the findings argue for a phenomenon, recently reported in myofibroblasts,[32] whereby a $[Ca^{2+}]_i$ transient–driven contractile force in one SMC is conveyed across well-developed adherens junctions to initiate a $[Ca^{2+}]_i$ transient in the adjacent cell. The second possibility is that the hybrid adherens junction served to facilitate gap-junction–mediated ion transfer. Importantly, SMC collectivization was associated with an accumulation of connexin 43–containing junctions at cell interfaces, and this proceeded in a cadherin-11– and N-cadherin–dependent manner. Thus, by bringing SMC surfaces together, gap-junction–mediated signaling between SMCs may have been enabled. The presence of phase-locked $[Ca^{2+}]_i$ oscillations is also consistent with gap-junction–mediated communication. Overall, the findings reveal a novel, communication role for cadherin-11–containing junctions in SMCs and elucidate a linkage between SMC cohesion and coordination of calcium signals.

In summary, the present report describes a novel, adhesive switching phenomenon for vascular SMCs. This switch is based on the rapid assembly and consolidation of adherens junctions and a previously unknown junction architecture, consisting of nanotracks of cadherin-11 and N-cadherin. This adhesive machinery, and the attendant formation of SMC networks, may contribute to stability and function of blood vessels.

Sources of Funding

This research was funded by the Canadian Institutes of Health Research (CIHR; FRN-11715 and FRN-126148), the Heart and Stroke Foundation of Canada (T7081), and the University of Western Ontario Department of Medicine (POEM). H. Yin was supported by a CIHR Fellowship. J. G. Pickering holds the Heart and Stroke Foundation of Ontario/Barnett-Ivey Chair.

Disclosures

None.

References

1. Clark JM, Glagov S. Transmural organization of the arterial media. The lamellar unit revisited. *Arteriosclerosis*. 1985;5:19–34.
2. Gown AM, Tsukada T, Ross R. Human atherosclerosis. II. Immunocytochemical analysis of the cellular composition of human atherosclerotic lesions. *Am J Pathol*. 1986;125:191–207.
3. Isner JM, Kearney M, Bauters C, Leclerc G, Nikol S, Pickering JG, Riessen R, Weir L. Use of human tissue specimens obtained by directional atherectomy to study restenosis. *Trends Cardiovasc Med*. 1994;4:213–221. doi: 10.1016/1050-1738(94)90037-X.
4. Pickering JG, Ford CM, Chow LH. Evidence for rapid accumulation and persistently disordered architecture of fibrillar collagen in human coronary restenosis lesions. *Am J Cardiol*. 1996;78:633–637.
5. Milewicz DM, Guo DC, Tran-Fadulu V, Lafont AL, Papke CL, Inamoto S, Kwartler CS, Pannu H. Genetic basis of thoracic aortic aneurysms and dissections: focus on smooth muscle cell contractile dysfunction. *Annu Rev Genomics Hum Genet*. 2008;9:283–302. doi: 10.1146/annurev.genom.8.080706.092303.
6. Rocnik E, Chow LH, Pickering JG. Heat shock protein 47 is expressed in fibrous regions of human atheroma and is regulated by growth factors and oxidized low-density lipoprotein. *Circulation*. 2000;101:1229–1233.
7. Pickering JG, Chow LH, Li S, Rogers KA, Rocnik EF, Zhong R, Chan BM. alpha5beta1 integrin expression and luminal edge fibronectin matrix assembly by smooth muscle cells after arterial injury. *Am J Pathol*. 2000;156:453–465.
8. Aalkjaer C, Nilsson H. Vasomotion: cellular background for the oscillator and for the synchronization of smooth muscle cells. *Br J Pharmacol*. 2005;144:605–616. doi: 10.1038/sj.bjp.0706084.
9. Alexander MR, Owens GK. Epigenetic control of smooth muscle cell differentiation and phenotypic switching in vascular development and disease. *Annu Rev Physiol*. 2012;74:13–40. doi: 10.1146/annurev-physiol-012110-142315.
10. Niessen CM, Leckband D, Yap AS. Tissue organization by cadherin adhesion molecules: dynamic molecular and cellular mechanisms of morphogenetic regulation. *Physiol Rev*. 2011;91:691–731. doi: 10.1152/physrev.00004.2010.
11. Takeichi M. Self-organization of animal tissues: cadherin-mediated processes. *Dev Cell*. 2011;21:24–26. doi: 10.1016/j.devcel.2011.06.002.
12. Sun Z, Parrish AR, Hill MA, Meininger GA. N-cadherin, a vascular smooth muscle cell-cell adhesion molecule: function and signaling for vasomotor control. *Microcirculation*. 2014;21:208–218. doi: 10.1111/micc.12123.
13. Uglow EB, Slater S, Sala-Newby GB, Aguilera-Garcia CM, Angelini GD, Newby AC, George SJ. Dismantling of cadherin-mediated cell-cell contacts modulates smooth muscle cell proliferation. *Circ Res*. 2003;92:1314–1321. doi: 10.1161/01.RES.0000079027.44309.53.
14. Sabatini PJ, Zhang M, Silverman-Gavrila R, Bendeck MP, Langille BL. Homotypic and endothelial cell adhesions via N-cadherin determine polarity and regulate migration of vascular smooth muscle cells. *Circ Res*. 2008;103:405–412. doi: 10.1161/CIRCRESAHA.108.175307.
15. Li S, Fan YS, Chow LH, Van Den Diepstraten C, van Der Veer E, Sims SM, Pickering JG. Innate diversity of adult human arterial smooth muscle cells: cloning of distinct subtypes from the internal thoracic artery. *Circ Res*. 2001;89:517–525.
16. van der Veer E, Nong Z, O'Neil C, Urquhart B, Freeman D, Pickering JG. Pre-B-cell colony-enhancing factor regulates NAD+-dependent protein deacetylase activity and promotes vascular smooth muscle cell maturation. *Circ Res*. 2005;97:25–34. doi: 10.1161/01.RES.0000173298.38808.27.
17. Frontini MJ, O'Neil C, Sawyez C, Chan BM, Huff MW, Pickering JG. Lipid incorporation inhibits Src-dependent assembly of fibronectin and type I collagen by vascular smooth muscle cells. *Circ Res*. 2009;104:832–841. doi: 10.1161/CIRCRESAHA.108.187302.
18. Frontini MJ, Nong Z, Gros R, Drangova M, O'Neil C, Rahman MN, Akawi O, Yin H, Ellis CG, Pickering JG. Fibroblast growth factor 9 delivery during angiogenesis produces durable, vasoresponsive microvessels wrapped by smooth muscle cells. *Nat Biotechnol*. 2011;29:421–427. doi: 10.1038/nbt.1845.
19. Kimura Y, Matsunami H, Inoue T, Shimamura K, Uchida N, Ueno T, Miyazaki T, Takeichi M. Cadherin-11 expressed in association with mesenchymal morphogenesis in the head, somite, and limb bud of early mouse embryos. *Dev Biol*. 1995;169:347–358. doi: 10.1006/dbio.1995.1149.
20. Hoffmann I, Balling R. Cloning and expression analysis of a novel mesodermally expressed cadherin. *Dev Biol*. 1995;169:337–346. doi: 10.1006/dbio.1995.1148.
21. Guerne PA, Lotz M. Interleukin-6 and transforming growth factor-beta synergistically stimulate chondrosarcoma cell proliferation. *J Cell Physiol*. 1991;149:117–124. doi: 10.1002/jcp.1041490115.
22. Tannenbaum JE, Waleh NS, Mauray F, Breuss J, Pytela R, Kramer RH, Clyman RI. Transforming growth factor beta 1 inhibits fetal lamb ductus arteriosus smooth muscle cell migration. *Pediatr Res*. 1995;37:561–570. doi: 10.1203/00006450-199505000-00001.
23. Duband JL, Dufour S, Hatta K, Takeichi M, Edelman GM, Thiery JP. Adhesion molecules during somitogenesis in the avian embryo. *J Cell Biol*. 1987;104:1361–1374.
24. Horikawa K, Radice G, Takeichi M, Chisaka O. Adhesive subdivisions intrinsic to the epithelial somites. *Dev Biol*. 1999;215:182–189. doi: 10.1006/dbio.1999.9463.
25. George SJ, Beeching CA. Cadherin:catenin complex: a novel regulator of vascular smooth muscle cell behaviour. *Atherosclerosis*. 2006;188:1–11. doi: 10.1016/j.atherosclerosis.2005.12.017.
26. Jackson TY, Sun Z, Martinez-Lemus LA, Hill MA, Meininger GA. N-cadherin and integrin blockade inhibit arteriolar myogenic reactivity but not pressure-induced increases in intracellular Ca. *Front Physiol*. 2010;1:165. doi: 10.3389/fphys.2010.00165.
27. Yap AS, Brieher WM, Pruschy M, Gumbiner BM. Lateral clustering of the adhesive ectodomain: a fundamental determinant of cadherin function. *Curr Biol*. 1997;7:308–315.
28. Monahan TS, Andersen ND, Panossian H, Kalish JA, Daniel S, Shrikhande GV, Ferran C, Logerfo FW. A novel function for cadherin 11/osteoblast-cadherin in vascular smooth muscle cells: modulation of cell migration and proliferation. *J Vasc Surg*. 2007;45:581–589. doi: 10.1016/j.jvs.2006.12.016.
29. Alimperti S, You H, George T, Agarwal SK, Andreadis ST. Cadherin-11 regulates both mesenchymal stem cell differentiation into smooth muscle cells and the development of contractile function in vivo. *J Cell Sci*. 2014;127(Pt 12):2627–2638. doi: 10.1242/jcs.134833.
30. Pittet P, Lee K, Kulik AJ, Meister JJ, Hinz B. Fibrogenic fibroblasts increase intercellular adhesion strength by reinforcing individual OB-cadherin bonds. *J Cell Sci*. 2008;121(Pt 6):877–886. doi: 10.1242/jcs.024877.
31. Massagué J. TGFβ signalling in context. *Nat Rev Mol Cell Biol*. 2012;13:616–630. doi: 10.1038/nrm3434.
32. Follonier L, Schaub S, Meister JJ, Hinz B. Myofibroblast communication is controlled by intercellular mechanical coupling. *J Cell Sci*. 2008;121(Pt 20):3305–3316. doi: 10.1242/jcs.024521.

Significance

Development of a cohesive smooth muscle cell network is critical to vascular stability and function. However, the basis for effective smooth muscle cell (SMC) network formation is not understood. This study identifies a molecular cascade by which SMCs can switch from semi-autonomous individuals to a functioning collective. This switch entails the assembly of a novel, strap-like adherens junction aggregate that is enriched in cadherin-11. Furthermore, using ground-state depletion microscopy, we have discovered an entirely new adherens junction architecture consisting of parallel nanotracks of cadherin-11 and N-cadherin. This cadherin assembly served not only to hold SMCs together but also to coordinate calcium transients among connected SMCs. These findings define a mechanism for the assembly of SMCs into communicating units, a process critical for the stability and function of blood vessels.